Journal of Electroanalytical Chemistry 688 (2013) 282–288

Contents lists available at SciVerse ScienceDirect

Journal of Electroanalytical Chemistry

journal homepage: www.elsevier.com/locate/jelechem

Polyphenazine films as inhibitors of copper corrosion

Andreia Romeiro, Carla Gouveia-Caridade, Christopher M.A. Brett *

Departamento de Química, Faculdade de Ciências e Tecnologia, Universidade de Coimbra, 3004-535 Coimbra, Portugal

ARTICLE INFO

Article history:
Available online 2 August 2012

Keywords:
Polyphenazine films
Redox polymer
Corrosion protective coatings
Copper
Electrochemical impedance spectroscopy

ABSTRACT

The polyphenazines poly(brilliant cresyl blue) (PBCB), poly(Nile blue A) (PNB) and poly(safranine T) (PST) have been investigated as corrosion protection films on copper electrodes by open circuit measurements, Tafel plots and electrochemical impedance spectroscopy, complemented by scanning electron microscopy. Pure copper electrodes were initially passivated in sodium oxalate or hydrogen carbonate solutions, to inhibit copper dissolution at potentials where phenazine monomer oxidation occurs, before electropolymerisation by potential cycling. The corrosion inhibition of these films was tested in 0.10 M KCl solution. It was found that, after long immersion times, the best protection efficiency was with PNB films formed on copper passivated in sodium hydrogen carbonate solution.

1. Introduction

Inhibition of corrosion phenomena is an important subject of intense investigation due to the large economic losses it causes worldwide [1]. The use of organic inhibitors is one of the most practical approaches for the corrosion protection of copper, involving the use of amines and azole derivatives containing nitrogen [2–10].

The remarkable physical and chemical properties of conducting polymers [11–16] have led to much research in different areas such as rechargeable batteries [11,12], sensors [13,14], molecular devices [17], energy storage systems [18] and membrane gas separation [19]. For corrosion protectors of oxidizable metals, conducting polymers have become of much interest. Deberry [20] first demonstrated that electrochemically synthesized polyaniline can act as a corrosion-protective layer on stainless steel in 1 M H_2SO_4. Since then many reports, e.g. [21–25] have investigated the performance of conducting polymer films as corrosion protectors.

During the last decade phenazine redox dyes have been used for the modification of electrode surfaces by electropolymerisation with a view to their possible use as redox polymers or redox mediators, many of the applications being related to the development of sensors and biosensors [26]. The electroactive properties of the monomers are usually retained upon polymerisation.

Brilliant cresyl blue (BCB) is a cationic quinine-imide dye with a planar and rigid structure as shown in Fig. 1a has been shown to possess promising properties as a redox catalyst. BCB can adsorb strongly on electrode surfaces and these chemically modified electrodes have been used for the determination of NADH [27] and to study the redox behaviour of haemoglobin [28], among other determinations, e.g. oxalate [29] and cyclodextrin [30] using spectrophotometric detection. Another application is as a mediator in electrochemical biosensors [31,32].

Nile blue (NB), a phenoxazine dye, Fig. 1b, is a well-known electroactive molecule. It has been use as a mediator of electron transfer with a two-electron redox conversion to modify solid electrodes for electrocatalytic oxidation of the reduced form of nicotinamide coenzymes NADH and NADPH [27,33,34].

Safranine T (ST), 3,7-diamino-2,8-dimethyl-5-phenylphenazinium chloride (Fig. 1c), is a water-soluble red-coloured phenazine-type dye used in the textile, pharmaceutical, paper and cosmetic industries [35] and as a marker in biological processes [36]. This dye, like many phenazine dyes, is difficult to degrade due to its complex structure and one of the ways to achieve this is electrochemical degradation [35]. The application of the dye monomer as a mediator in a biosensing system with nitrite and nitrate reductase has been reported [37].

In previous work [38], films of the phenazine polymer poly(neutral red) have been demonstrated to inhibit copper corrosion in 0.1 M KCl. In this work, the polyazines PBCB, PNB and PST will be investigated for possible corrosion protection of copper using open circuit potential measurements, Tafel plots and electrochemical impedance spectroscopy in 0.1 M KCl.

2. Experimental

2.1. Reagents and solutions

Electrolytes used for passivation of copper were 0.125 M sodium oxalate pH 6.85 ($C_2Na_2O_4$, Merck) and 0.10 M sodium hydrogen carbonate pH 8.35 ($NaHCO_3$, Riedel-de Haën, Germany).

* Corresponding author. Tel.: +351 239835295; fax: +351 239827703.
E-mail address: brett@ci.uc.pt (C.M.A. Brett).

1572-6657/$ - see front matter © 2012 Elsevier B.V. All rights reserved.
http://dx.doi.org/10.1016/j.jelechem.2012.07.033

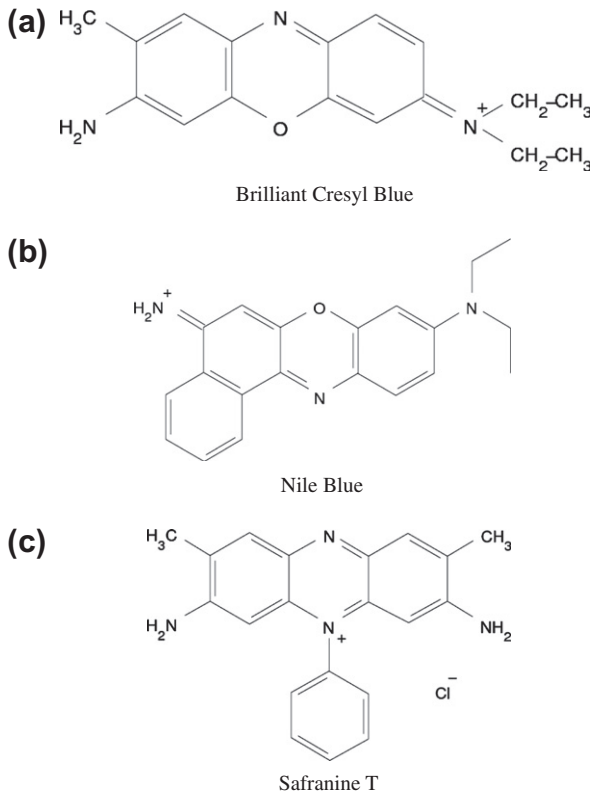

Fig. 1. Chemical structure of: (a) brilliant cresyl blue, (b) Nile blue and (c) safranine T.

Brilliant cresyl blue (BCB) was from Fluka, USA and Nile blue A (NB) was from Fluka, France. The correct amount of each monomer to prepare a solution of 0.5 mM was dissolved in 0.10 M sodium phosphate buffer (NaPB) pH 8.2 prepared from di-sodium hydrogen phosphate dihydrate ($Na_2HPO_4{\cdot}2H_2O$, Fluka, Germany) and sodium dihydrogen phosphate hydrate ($NaH_2PO_4{\cdot}H_2O$, Riedel-de Haën, Germany).

Safranine T (ST) was obtained from La Chema, Czech Republic. A 0.5 mM ST solution was prepared in 0.025 M potassium phosphate buffer (KPB) pH 5.54 prepared from di-potassium hydrogen phosphate trihydrate ($K_2HPO_4{\cdot}3H_2O$, Panreac, Spain) and potassium dihydrogen phosphate (KH_2PO_4, Riedel-de Haën, Germany).

Corrosion tests were carried out in 0.10 M potassium chloride (KCl, Fluka). Millipore Milli-Q nanopure water (resistivity >18 MΩ cm) was used for preparation of all solutions. All experiments were performed at 24 ± 1 °C.

2.2. Electrode preparation

The electrodes used were made from copper cylinders (99.99% purity Goodfellow Metals, Cambridge, UK) by sheathing in glass and epoxy resin. The exposed disc electrode surface area was 0.20 cm^2. Before experiments, the electrodes were mechanically abraded with 400, 600, 800 and 1500 grade silicon carbide papers. After this polishing procedure, the electrodes were cleaned with water.

2.3. Instrumentation

Experiments were conducted in a three electrode cell using a modified or unmodified copper working electrode, a saturated calomel electrode (SCE) as reference and platinum foil as counter electrode.

Cyclic voltammetry was carried out using a potentiostat/galvanostat (Autolab PGSTAT30) connected to a computer with general purpose electrochemical system software (GPES V4.9) from Metrohm-Autolab (Utrecht, Netherlands).

Electrochemical impedance spectroscopy was carried out on a PC-controlled Solartron 1250 frequency response analyzer, coupled to a Solartron 1286 electrochemical interface using ZPlot 2.4 software (Solartron Analytical, UK), with a rms perturbation of 10 mV applied over the frequency range 65.5 kHz–0.01 Hz, with 10 frequency values per decade.

Microscope images of polymer coated passivated copper electrodes were acquired using a scanning electron microscope (SEM) Jeol JSM-5310 (Jeol, Tokyo, Japan), equipped with a thermionic field emission SEM and an electronically controlled automatic gun. The images were captured at 10 kV.

2.4. Cu electrode passivation and modification with PBCB, PNB and PS

Copper electrodes were first passivated by potential cycling from −0.5 V to +1.0 V vs SCE and −1.0 V to + 0.75 V vs SCE in sodium oxalate and sodium hydrogen carbonate solutions, respectively, during five cycles at a scan rate of 20 mV s^{-1}, potential limits optimised in previous work in order to avoid hydrogen evolution and limit oxygen evolution [38].

The polymer films were prepared by electropolymerisation of their monomers from an aqueous solution of 0.5 mM BCB or NB in 0.1 M NaPB pH 8.2, cycling the potential from –1.0 V to +0.5 V vs SCE for electrodes passivated in sodium oxalate, −1.0 V to +0.75 V vs SCE for electrodes passivated in sodium hydrogen carbonate, during 20 cycles at a potential sweep rate of 20 mV s^{-1}. The PST film was prepared by electropolymerisation from an aqueous solution of 0.5 mM safranine T in 0.025 M KPB pH 5.54 by cycling the potential from −0.8 V to +0.5 V vs SCE for electrodes passivated in sodium oxalate and −0.6 V to +0.3 V vs SCE for electrodes passivated in sodium hydrogen carbonate, during 20 cycles at a scan rate of 20 mV s^{-1}.

3. Results and discussion

3.1. Electropolymerisation

Before electropolymerisation of BCB, NB and ST, the Cu electrodes were passivated by potential cycling in sodium oxalate and sodium hydrogen carbonate solutions. The passivation of copper was necessary because oxidation of the phenazine monomers occurs at potentials where dissolution of copper takes place, this thus being prevented, and also to ensure surface roughening to promote better adhesion of the polymer film to the copper substrate.

The passivation of copper in oxalate and hydrogen carbonate solutions has already been studied [39–45] and a summary can be found in [38]; the passivated electrode will be referred to as Cu/oxalate or Cu/$Na_2C_2O_4$ and as Cu/hydrogen carbonate or Cu/$NaHCO_3$ below. The formation of the polymer films on passivated copper electrodes was carried out by electropolymerisation of the monomer using potential cycling, as described in the experimental section. The mechanism of polymerisation involves initiation by formation of a cation-radical upon electrooxidation [46].

Fig. 2 shows cyclic voltammograms obtained during the formation of PBCB, PNB and PST films on the passivated Cu electrodes in sodium oxalate (Fig. 2a) and sodium hydrogen carbonate (Fig. 2b) solutions. In the case of the formation of PBCB, it can be observed that the irreversible oxidation of monomer occurs at ∼+0.5 V and ∼+0.75 V vs SCE on Cu/oxalate and Cu/hydrogen carbonate, respectively. A redox couple appears at ∼−0.3 V in Cu/oxalate and ∼−0.4 V vs SCE in Cu/hydrogen carbonate (calculated as the

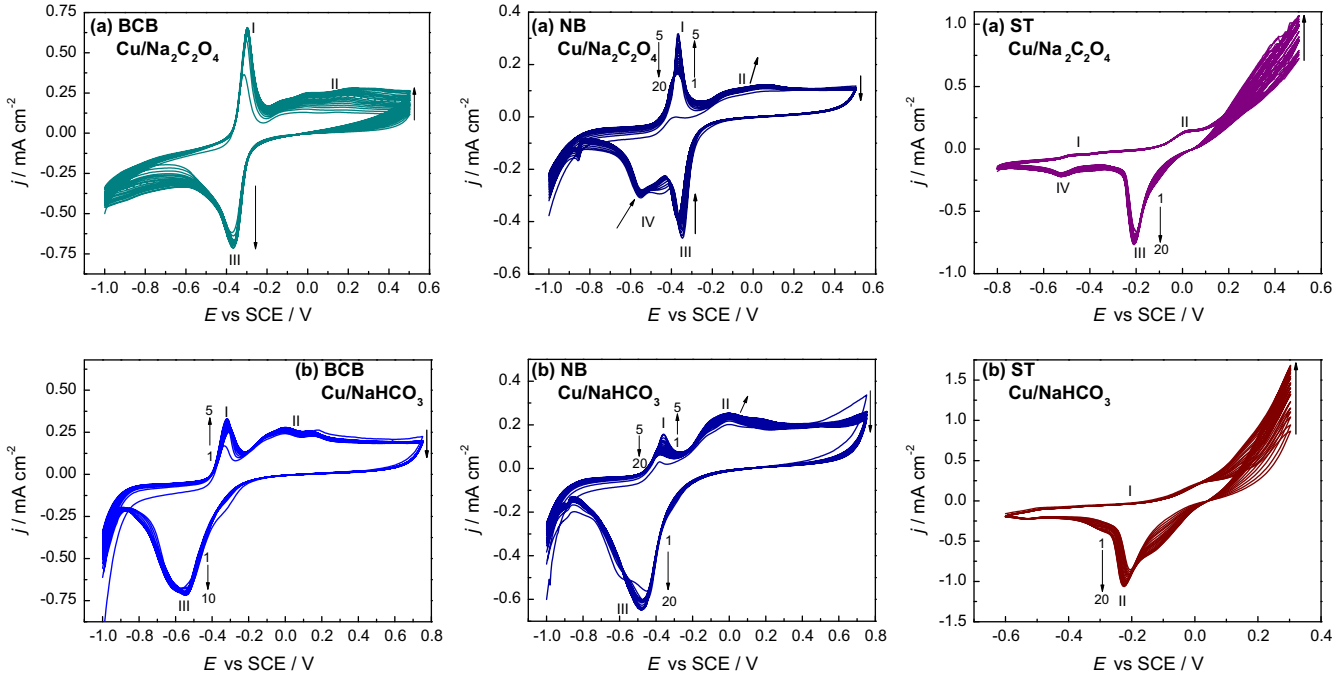

Fig. 2. Cyclic voltammograms of the electropolymerisation of BCB, NB and ST on passivated copper electrodes in (a) sodium oxalate and (b) sodium hydrogen carbonate solutions.

midpoint between the oxidation and reduction peak potentials) corresponding to oxidation/reduction of the monomer. For Cu/$Na_2C_2O_4$, the increase in peak II and in peak III height, with a small shift to more negative potentials confirms the deposition of the PBCB film. For Cu/hydrogen carbonate, the increase in peak I and II up until cycle number 5, reveals film formation.

During electropolymerisation of NB, the redox peaks corresponding to redox reaction of NB monomer, ~+0.5 V and ~+0.75 V vs SCE on Cu/oxalate and Cu/hydrogen carbonate electrodes, decrease quickly with the increase of the number of cycles. A new redox couple appears around 0.0 V vs SCE in the cyclic voltammogram. According to Cai et al. [47] the redox couple I/IV in Cu/oxalate can be attributed to the redox reaction of the conjugated structure of the NB monomer on the surface of the polymer structure, and the redox couple II/III to the oxidation/reduction reaction of the polymer (and in Cu/hydrogen carbonate redox couple I/III). Since PNB films act as a semi-conductor [48], thicker and more compact films may make the electron transfer more difficult, leading to the observed decrease of the peak currents.

In the case of the electropolymerisation of ST in Cu/oxalate, two redox couples and one irreversible oxidation are observed. The first redox couple at ~−0.5 V vs SCE, peaks I/IV, is attributed to the redox process for ST_{ox}/ST_{red}, as found for ST and neutral red electropolymerisation on carbon film electrodes [49]. The other redox couple, peaks II/III, is due to doping and dedoping of the film. These peaks increased in height with increase in the number of cycles which confirms film formation. On Cu/hydrogen carbonate the increase in peak II is more visible, with a small shift to more negative potentials due to the PST conformation and/or counterion diffusion limitations, like that observed for PNR formation on passivated copper [38].

3.2. Electrochemical studies of polymer-coated passivated copper corrosion

3.2.1. Open circuit potential (OCP)

Open circuit potential measurements were made on modified passivated copper electrodes with PBCB, PNB and PST films in 0.10 M KCl electrolyte solution during 4 h of immersion. The results are shown in Fig. 3a and b for electrodes passivated in sodium oxalate and sodium hydrogen carbonate solutions, respectively. For comparison the OCP for bare copper electrodes and after passivation is also plotted.

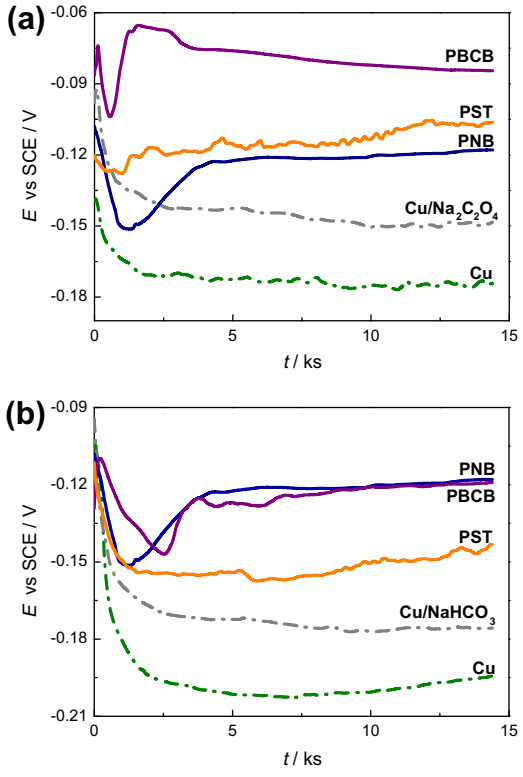

Fig. 3. Open circuit potential vs time plots in 0.1 M KCl of bare copper, copper passivated in (a) sodium oxalate and (b) sodium hydrogen carbonate solutions and after posterior modification with PBCB, PNB or PST.

It can be seen that the OCP values after 4 h immersion in 0.10 M KCl solution are more positive for the polymers electrodeposited on oxalate-passivated copper electrodes, They are more positive than the OCP for bare copper electrodes, and also more positive than for oxalate passivated or hydrogen carbonate passivated Cu electrodes, showing that these polymers can be used as protective corrosion layers on copper.

During the first seconds of immersion of the PBCB and PNB modified electrodes the OCP decreases after which it increases rapidly, continuing to increase until ~4000 s, where it tends to stabilise. The initial decrease in the potential can be ascribed to diffusion of chloride ions through the pores of the polymer films.

In the case of PST modified passivated copper electrodes, the OCP initially decreases and then tends to stabilize, although with small fluctuations, and the potential was not yet completely stable after 4 h.

The OCP is more positive for the electrodes previously passivated in oxalate and then modified with PBCB. Considering the electrodes passivated in hydrogen carbonate the OCP profile is similar for Cu/$NaHCO_3$/PBCB and Cu/ $NaHCO_3$/PNB, overlapping after ~8000 s.

All three polymers presented more positive OCP values than those obtained with PNR modified passivated copper electrodes [38], with more rapid stabilisation of the OCP curves.

3.2.2. Tafel polarization plots

Tafel plots, Fig. 4, were obtained after immersion of the copper electrodes modified with PBCB, PNB and PST for 4 h in 0.10 M KCl. The parameters obtained from analysis of these plots are presented in Table 1. Values for bare copper and copper passivated in oxalate and hydrogen carbonate are also shown, taken from [38].

Taking into consideration that the passive film and the polymer films are electrochemically inert at low anodic overpotential, the porosities of the films were calculated using the expression used by Shinde [41]:

$$P = \left(\frac{R_{ps}}{R_{pc}}\right) \times 10^{-(\Delta E_{cor}/\beta_a)} \quad (1)$$

where P is the total coating porosity, R_{ps} and R_{pc} are the polarization resistances, R_p, of the bare copper and the modified copper electrode, ΔE_{cor} is the difference potential between the corrosion potential of modified copper and bare copper electrode, and β_a is the anodic Tafel coefficient for bare copper.

The porosities decrease after modification of passivated copper with polymer coatings except in the case of Cu/$NaHCO_3$/PST, where the porosity is higher than Cu/$NaHCO_3$. In increasing order, the values of porosity were:

Oxalate passivated Cu: Cu/$Na_2C_2O_4$/PBCB < Cu/$Na_2C_2O_4$/PST < Cu/$Na_2C_2O_4$/PNB.
Hydrogen carbonate passivated Cu: Cu/$NaHCO_3$/PBCB < Cu/$NaHCO_3$/PNB < Cu/$NaHCO_3$/PST.

The film with lowest porosity was PBCB electrodeposited in Cu/$Na_2C_2O_4$ with 0.01% of total porosity, and that with highest porosity was PST electrodeposited in Cu/$NaHCO_3$ with 11.7%.

The protection efficiency (PE%) values were estimated using the following equation, as in [41]

$$PE\% = \left(\frac{R_{pc} - R_{ps}}{R_{pc}}\right) \times 100 \quad (2)$$

where R_{ps} and R_{pc} have the same meaning as in Eq. (1). The values obtained are given in Table 1.

The best efficiency was obtained with PNB deposited on the passivated copper electrode in sodium hydrogen carbonate solution (~82.7%); no inhibition was obtained with PBCB films either deposited on top of Cu/$Na_2C_2O_4$ or on Cu/$NaHCO_3$.

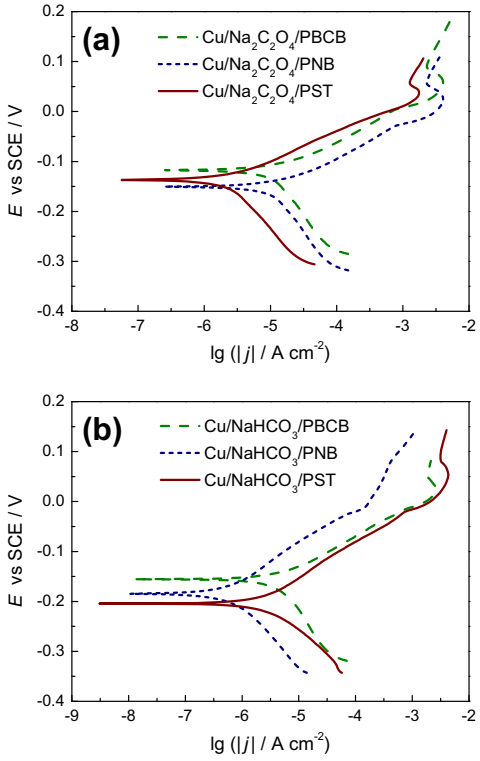

Fig. 4. Tafel plots after 4 h immersion in 0.10 M KCl of PBCB, PNB and PST on (a) sodium oxalate and (b) sodium hydrogen carbonate passivated copper electrodes.

Comparing the polarization resistance for electrodes modified with PBCB either in Cu/$Na_2C_2O_4$ or in Cu/$NaHCO_3$ with unmodified copper, the R_p values are lower than for the unmodified copper (2.8 kΩ cm^2). Although the OCP is more negative with the PBCB coating, the current corrosion density is higher, leading to faster corrosion for Cu/$Na_2C_2O_4$/PBCB and Cu/$NaHCO_3$/PBCB than in the case of the unmodified electrode. This may also be due to poor adhesion of PBCB films on the passivated electrodes, and also to leaching of the film during recording of polarization curves. The polarization resistance is higher for Cu/$NaHCO_3$/PNB, which also means higher protection efficiency, 82.7%. This protection efficiency is also higher than that with PNR in the system Cu/$NaHCO_3$/PNR, ~68% [38].

The results obtained from open circuit measurements and Tafel plots are in agreement, some difference between E_{cor} and OCP being due to polarisation effects.

Table 1
Data from Tafel plots for different modified copper electrodes after4 h immersion in 0.10 M KCl.

Electrode assembly	R_p (kΩ cm^2)	E_{corr} (V (SCE))	β_a (V dec^{-1})	$\lvert\beta_c\rvert$ (V dec^{-1})	P (%)	PE (%)
Bare Cu[a]	2.77	−0.221	0.023	0.018		
Cu/$Na_2C_2O_4$[a]	3.99	−0.167	0.048	0.034	0.31	30.6
Cu/$Na_2C_2O_4$/PBCB	0.85	−0.118	0.053	0.032	0.01	–
Cu/$Na_2C_2O_4$/PNB	4.10	−0.149	0.060	0.033	0.05	32.4
Cu/$Na_2C_2O_4$/PST	3.90	−0.147	0.068	0.036	0.04	28.9
Cu/$NaHCO_3$[a]	4.57	−0.190	0.021	0.024	2.7	39.4
Cu/$NaHCO_3$/PBCB	1.80	−0.156	0.036	0.026	0.23	–
Cu/$NaHCO_3$/PNB	16.0	−0.180	0.042	0.039	0.29	82.7
Cu/$NaHCO_3$/PST	4.30	−0.204	0.038	0.046	11.7	35.6

[a] Values from [38].

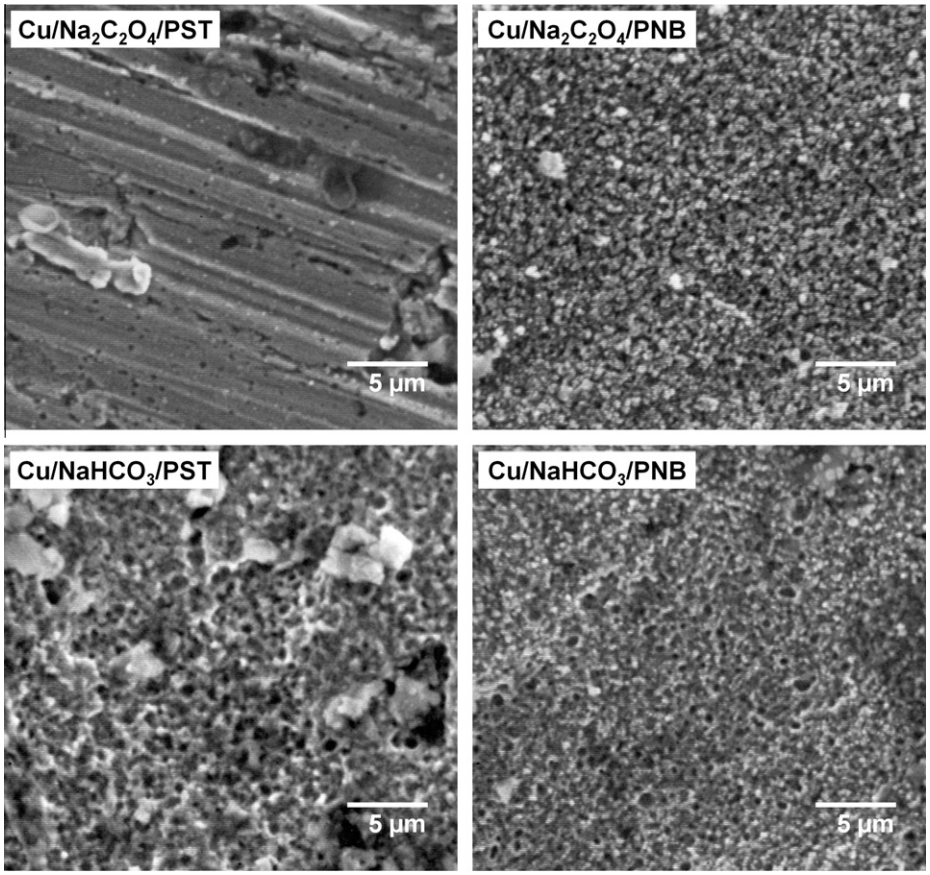

Fig. 5. Scanning electron micrographs of PST and PNB electrodeposited on Cu/oxalate and Cu/hydrogen carbonate.

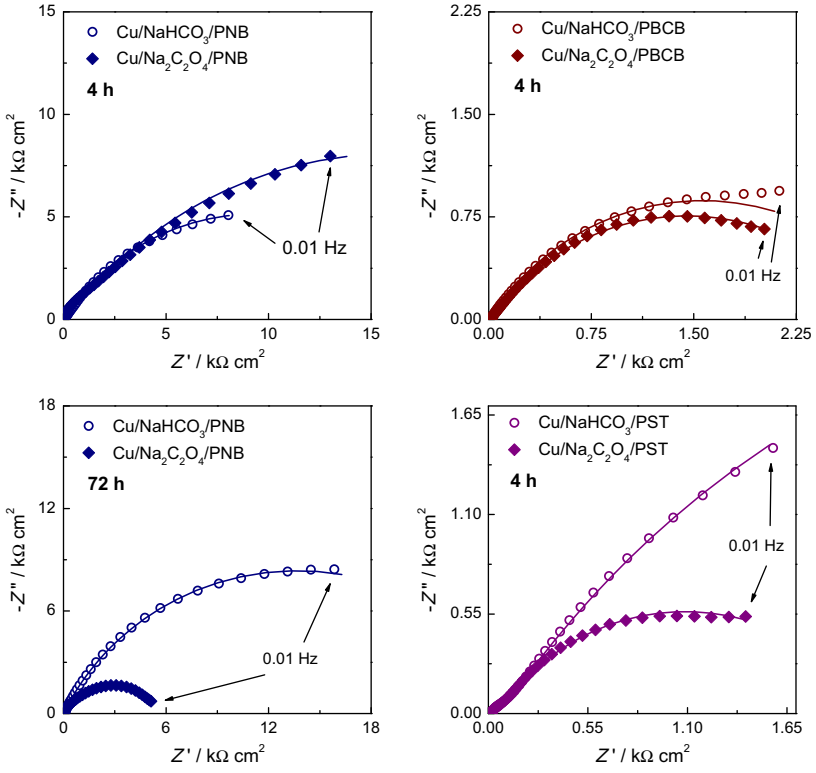

Fig. 6. Complex plane impedance plots of Cu modified electrodes after immersion in 0.10 M KCl. Lines denote the data fitting to the equivalent electrical circuit.

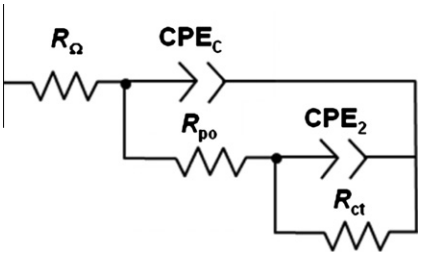

Fig. 7. Equivalent electrical circuit used for modelling the impedance spectra in Fig. 6.

3.3. Scanning electron microscopy (SEM)

The surface morphologies of the films were studied by SEM. In general terms, the porosity data obtained from Tafel plots are in agreement with what is observed from SEM images.

Representative images of PST and PNB films on Cu/oxalate and Cu/hydrogen carbonate are presented in Fig. 5. These images were chosen due to the higher porosity obtained from Tafel plots data for Cu/hydrogen carbonate/PST (11.7%), and the best anti-corrosive performance of Cu/hydrogen carbonate/PNB. It can be seen that in the case of passivated copper in sodium hydrogen carbonate the PST film has some non-conductive particles of ~100 nm diameter distributed all over the passivated copper surface. The image with PNB on Cu/hydrogen carbonate also has these non-conductive particles, but in lower number, so they are probably oxide formed during passivation, In the case of PST and PNB on Cu/oxalate, the surface is completely covered by the film, which is more visible on Cu/oxalate/PNB. It also has non-conductive particles in clusters, as well as holes distributed all over the surface. The differences between the morphologies of films can also be attributed to the different morphologies of the copper oxide layers obtained in oxalate and hydrogen carbonate passivation solutions.

3.4. Electrochemical impedance spectroscopy

Polarization curve analyses revealed that only the PNB coating gave a significant protection against the corrosion of copper. Electrochemical impedance spectroscopy was employed to test the stability behaviour of the PNB films on passivated copper electrodes. Fig. 6 shows complex plane impedance spectra in 0.10 M KCl at the open circuit potential after 4 and 72 h immersion for the PNB-coated passivated copper electrode. For $Cu/NaHCO_3$, the spectra after 4 and 72 h immersion are almost the same, which can be attributed to a stable film.

For comparison, spectra obtained for PBCB and PST-coated Cu passivated electrode after 4 h immersion in 0.10 M KCl are also presented, although with these two polymers the protection efficiency calculated from Tafel plots was much less good. This is reflected in the lower magnitude of the impedance values. by almost a factor of ten.

The spectra were fitted to the equivalent electrical circuit in Fig. 7. This circuit comprises the cell resistance R_Ω in series with a constant phase element CPE_c representing the coating capacitance, C_c connected in parallel with the coating pore resistance R_{po}. This resistance is also in series with another RCPE combination with R_{ct} the charge transfer resistance describing the corrosion processes in the bottom of the pores of the passivated copper and CPE_2 the capacitance of the passivated copper surface inside the pores, C_2. This equivalent electrical circuit is the same used for analysed the impedance data obtained with poly(neutral red) coatings electrochemically deposited in passivated copper electrodes [38] and already used in studies with other polymers coated metals in corrosive electrolytes [22–25]. As in [38], the characteristics of the polymer films are given at high frequencies by the resistance R_{po}, related to the pore resistance of the coating from penetration of the electrolyte under the coating, the polymer coating, and the coating capacitance C_c. The other combination $R_{ct}CPE_2$ is associated with the characteristics of the electrolyte/copper interface on the bottom of the pores, appearing at low frequencies. The CPE, used due to the heterogeneity of the polymer coatings, models a non-ideal capacitor of capacitance C with a roughness factor α and is given by the expression $CPE = \{(C\,i\omega)^{\alpha}\}^{-1}$.

Table 2 summarizes the values of the parameters obtained from the fitting after different immersion times for PNB coated Cu passivated electrodes. For comparison, Table 2 also summarizes the parameters from spectra obtained after 4 h immersion for PBCB and PST coated passivated Cu. The errors in the fitting of the experimental values to the equivalent circuit varied between 2% and 13% for resistances R_{po} and R_{ct}, 1–6% for capacitances C_c and C_2, and ~1% for α_1 and α_2. It is suggested in [41] that the sum $R_{po} + R_{ct}$ can be correlated with R_{pol} from polarization experiments. Examination of Table 1 and 2 suggests that the trends are the same but numerical values are rather different, reflecting the different experimental conditions under which measurements are made.

The cell resistance was almost invariant with time of immersion of the electrodes in 0.10 M KCl and with the passivation solution or PNB coated electrode with a value of 14.4 ± 0.7 Ω cm^2.

The pore resistance is higher for the $Cu/Na_2C_2O_4$/PNB with the highest R_{po} obtained for 24 h immersion (4073 Ω cm^2), decreasing after this. In contrast, for $Cu/NaHCO_3$/PNB R_{po} increases during the whole 72 h of the experiment, which can be attributed to the covering of the pores by corrosion products. Such an increase of R_{po} with time was already observed with poly(neutral red) coated passivated copper electrodes in sodium oxalate and sodium hydrogen carbonate solutions [38]. There is also an increase in the coating capacitance C_c on the $Cu/ NaHCO_3$/PNB electrode with time which

Table 2
Data obtained from analysis of the impedance spectra of Fig. 6.

Electrode assembly	Immersion time (h)	R_{po} (Ω cm^2)	C_c (μF cm^{-2})	α_1	R_{ct} (kΩ cm^2)	C_2 (μF cm^{-2})	α_2
$Cu/Na_2C_2O_4$/PBCB	4	46.0	16.1	0.90	2.90	223	0.60
$Cu/NaHCO_3$/PBCB	4	3100	214	0.68	–	–	–
$Cu/ Na_2C_2O_4$/PST	4	67.0	23.7	0.87	2.10	373	0.62
$Cu/NaHCO_3$/PST	4	97.3	42.3	0.86	8.90	503	0.61
$Cu/ Na_2C_2O_4$/PNB	4	1439	5.74	0.94	30.5	5.22	0.59
	24	4073	6.57	0.93	16.9	9.52	0.67
	48	2202	9.70	0.89	8.36	23.3	0.65
	72	924	10.4	0.88	4.67	48.4	0.65
$Cu/NaHCO_3$/PNB	4	240	12.3	0.84	18.5	80.5	0.62
	24	469	15.6	0.82	25.6	27.5	0.61
	48	595	17.4	0.80	27.4	22.2	0.59
	72	841	20.4	0.78	27.1	19.2	0.58

can be attributed to water uptake by the polymer. The charge transfer resistance for $Cu/NaHCO_3$/PNB increases with immersion time, leading to the conclusion that PNB coatings on a passivated copper electrode in sodium hydrogen carbonate solution have a better performance as anti corrosive agent on passivated copper surfaces. It is also seen that PNB deposited on $Cu/NaHCO_3$ has a very good anti-corrosion efficiency, with a charge transfer resistance of 27.1 $k\Omega\,cm^2$ after 72 h immersion in 0.10 M KCl, whereas PNR deposited on $Cu/Na_2C_2O_4$, has an R_{ct} of only 3.8 $k\Omega\,cm^2$ [38] after 72 h immersion (PNR deposited on $Cu/Na_2C_2O_4$ was found to be the best coating for corrosion protection of Cu in [38]). The higher efficiency of the PNB coatings is probably linked to the different monomer structure which leads to a more compact morphology, as discussed above.

In the case of the other two polymers, PBCB and PST, after 4 h immersion in 0.10 M KCl the R_{po} and R_{ct} values are very low compared with those obtained with PNB coatings, in agreement with the data obtained from Tafel plots and to the lower efficiency of these coatings in the corrosion protection of copper.

4. Conclusions

Brilliant cresyl blue, Nile blue and safranine T have been electropolymerised on copper electrodes by potential cycling. The electrodes were first passivated in sodium oxalate and sodium hydrogen carbonate solutions, due to Cu dissolution at potentials where the monomers BCB, NB and ST are oxidised to start their polymerisation at the electrode.

The anti-corrosion behaviour of the films was investigated in 0.10 M KCl using open circuit potential measurements, Tafel plots and electrochemical impedance spectroscopy complemented by scanning electron microscopy. The protection efficiency calculated from Tafel plots after 4 h of immersion in 0.10 M KCl was higher for the PNB coating deposited on Cu passivated in sodium hydrogen carbonate solution (Cu/hydrogen carbonate/PNB) with 82.7%, and a polarization resistance of 16.0 $k\Omega\,cm^2$. EIS confirms the best anti-corrosive behaviour of PNB films in $Cu/NaHCO_3$ electrodes, leading to the conclusion that PNB improves the corrosion behaviour of copper electrodes, more than the other polyphenazines. Further research on reducing film porosity to improve the protection efficiency will be carried out in the future.

Acknowledgements

Financial support from Fundação para a Ciência e a Tecnologia (FCT), Portugal PTDC/QUI/65732/2006, PTDC/QUIQUI/116091/2009, POCI 2010, POPH and COMPETE (co-financed by the European Social Fund FSE) and CEMUC® (Research Unit 285), Portugal, is gratefully acknowledged. CGC thanks FCT for postdoctoral fellowship SFRH/BPD/46635/2008.

References

[1] E.M. Sherif, S.M. Park, J. Electrochem. Soc. 152 (2005) B 428.
[2] E. Geler, D.S. Azambuja, Corros. Sci. 42 (2000) 631.
[3] E.M. Sherif, S.M. Park, Electrochim. Acta 51 (2006) 6556.
[4] M. Scendo, Corros. Sci. 49 (2007) 373.
[5] E.M. Sherif, R.M. Erasmus, J.D. Comins, Corros. Sci. 50 (2008) 3439.
[6] E.M. Sherif, R.M. Erasmus, J.D. Comins, J. Colloid Interface Sci. 311 (2007) 144.
[7] E.M. Sherif, S.M. Park, Corros. Sci. 48 (2006) 4065.
[8] K. Babic-Samardzija, C. Lupu, N. Hackerman, A.R. Barron, A. Luttge, Langmuir 21 (2005) 12187.
[9] M. Behpour, S.M. Ghoreishi, M. Salavati-Niasari, B. Ebrahimi, Mater. Chem. Phys. 107 (2008) 153.
[10] E. Abelev, D. Starosvetsky, Y. Ein-Eli, Langmuir 23 (2007) 11281.
[11] H.K. Song, G. Palmore, R. Tayhas, Adv. Mater. 18 (2006) 1764.
[12] Z. Cai, M. Geng, Z. Tang, J. Mater. Sci. 39 (2004) 4001.
[13] R.M. Rosa, R.L. Szulc, R.W.C. Li, J. Gruber, Macromol. Symp. 229 (2005) 138.
[14] P.P. Sengupta, S. Barik, B. Adhikari, Mater. Manufact. Processes 21 (2006) 263.
[15] Y. Wang, X. Jing, Polym. Adv. Technol. 16 (2005) 344.
[16] X. Jing, Y. Wang, B. Zhang, J. Appl. Polym. Sci. 98 (2005) 2149.
[17] V. Saxena, B.D. Malhotra, Curr. Appl. Phys. 3 (2003) 293.
[18] M. Arulepp, L.J. Permann, J. Power Sources 133 (2004) 320.
[19] J. Mansouri, R.P. Burford, J. Membr. Sci. 87 (1994) 23.
[20] D.W. Deberry, J. Electrochem. Soc. 132 (1985) 1022.
[21] G. Bereket, E. Hur, Y. Sahin, Prog. Org. Coat. 54 (2005) 63.
[22] D. Huerta-Vilca, B. Siefert, S.R. Moraes, M.F. Pantoja, A. Motheo, Mol. Cryst. Liq. Cryst. 415 (2004) 229.
[23] V. Shinde, S.R. Sainkar, P.P. Patil, Corros. Sci. 47 (2005) 1352.
[24] W.S. Araujo, I.C.P. Margarit, M. Ferreira, O.R. Mattos, P. Neto, Electrochim. Acta 46 (2001) 1307.
[25] J.O. Iroh, W. Su, Electrochim. Acta 46 (2000) 15.
[26] R. Pauliukaite, M.E. Ghica, M.M. Barsan, C.M.A. Brett, Anal. Lett. 43 (2010) 1588.
[27] B. Persson, L. Gorton, J. Electroanal. Chem. 292 (1990) 115.
[28] S. Dong, Y. Zhu, S. Song, Bioelectrochem. Bioenerg. 21 (1989) 233.
[29] A. Kazemzadeh, F. Moztarzadeh, Sens. Actuators B 106 (2005) 832.
[30] Q.-F. Zhang, Z.-T. Jiang, Y.-X. Guo, R. Li, Spectrochim. Acta A 69 (2008) 65.
[31] M.J. Lobo, A.J. Miranda, P. Tuñon, Electroanalysis 8 (1996) 591.
[32] R. Mieliauskiene, M. Nistor, V. Laurinavicius, E. Csöregi, Sens. Actuators B113 (2006) 671.
[33] F. Ni, H. Feng, C. Gorton, T.M. Cotton, Langmuir 6 (1990) 66.
[34] H.X. Ju, L. Dong, H.Y. Chen, Chem. J. Chin. Univ. 16 (1995) 1200.
[35] H.W. Gao, J.F. Zhao, J. Trace Microprobe Techn. 21 (2003) 615.
[36] B. Sterliz, B. Gründig, K.D. Vorlop, P. Bartholmes, H. Kotte, U. Stottmeister, Fresenius J. Anal. Chem. 349 (1994) 676.
[37] K.M. O'Connell, E. Waldner, L. Rouillier, E. Laviron, J. Electroanal. Chem. 162 (1984) 77.
[38] A. Romeiro, C. Gouveia-Caridade, C.M.A. Brett, Corros. Sci. 53 (2011) 3970.
[39] A.C. Cascalheira, L.M. Abrantes, Electrochim. Acta 49 (2004) 5023.
[40] A.C. Cascalheira, S. Aeiyach, J. Aubard, P.C. Lacaze, L.M. Abrantes, Russ. J. Electrochem. 40 (2004) 294.
[41] V. Shinde, P.P. Patil, Mat. Sci. Eng. B – Solid 168 (2010) 142.
[42] S. González, M. Pérez, M. Barrera, A.R.G. Elipe, R.M. Souto, J. Phys. Chem. B102 (1998) 5483.
[43] M.P. Sánchez, R.M. Souto, M. Barrera, S. González, R.C. Salvarezza, A. Arvia, Electrochim. Acta 38 (1993) 703–715.
[44] S. Patil, S.R. Sainkar, P.P. Patil, Appl. Surf. Sci. 225 (2004) 204.
[45] A.T. Ozyilmaz, T. Tuken, B. Yazici, M. Erbil, Prog. Org. Coat. 52 (2005) 92.
[46] A.A. Karyakin, E.E. Karyakina, H.L. Schmidt, Electroanalysis 11 (1999) 149.
[47] P.D. Du, S. Liu, P. Wu, C.X. Cai, Electrochim. Acta 53 (2007) 1811.
[48] J.M. Bauldreay, M.D. Archer, Electrochim. Acta 28 (1983) 1515.
[49] R. Pauliukaite, A. Selskiene, A. Malinauskas, C.M.A. Brett, Thin Solid Films 517 (2009) 5435.